Quantifying Uncertainties in the Performance Prediction of Existing Concrete Structures using an Extended Direct Stiffness Method Approach

Stef Helderweirt
PhD researcher, Dept. of Structural Eng. and Building Materials, Ghent University, Ghent, Belgium

Karel Van Den Hende
PhD researcher, Dept. of Structural Eng. and Building Materials, Ghent University, Ghent, Belgium

Wouter Botte
Post-Doctoral researcher, Dept. of Structural Eng. and Building Materials, Ghent University, Ghent, Belgium

Els Verstrynge
Professor, Dept. of Civil Engineering, KU Leuven, Leuven, Belgium

Robby Caspeele
Professor, Dept. of Structural Eng. and Building Materials, Ghent University, Ghent, Belgium

ABSTRACT: New construction rates in industrialized countries stagnate while refurbishment and retrofitting of existing concrete structures gain in importance. In order to be able to accurately predict the structural performance of these concrete structures, a DSM tool for daily engineering practice is constructed, based on the Direct Stiffness Method. In this contribution, a probabilistic analysis is performed with this DSM tool. The typical uncertainties involved with existing concrete structures are accounted for and it is investigated how they propagate to the outputs, i.e. deformations, internal forces etc. Furthermore, a parameter study is performed on the spatial correlation structure. The application on a frame structure shows that changing the correlation length and correlation coefficients of the corrosion parameters has a limited influence on the reliability index of the most critical element for flexural failure. Lastly, a sensitivity analysis is performed on the input variables, showing that the concrete tensile strength and the applied load have the highest influence on the midspan deflection of the frame. Moreover, as the structure deteriorates, the corrosion variables seem to significantly increase in importance.

1. INTRODUCTION

Reinforced concrete (RC) structures are widely used in many industrialized countries. Currently, significant parts of the patrimony in these regions are reaching the end of their lifetime. As a result, the through-life analysis of existing structures based on quantitative data is rapidly gaining attention. An essential part of this analysis is the performance prediction of existing concrete structures taking time-dependent degradation effects into account, which can be modelled by extending the Direct Stiffness Method (DSM). The constructed DSM tool is a second order, non-linear finite element model, which is able to incorporate several corrosion effects, such as a reduction of steel area, concrete cracking and spalling, a reduced steel ductility and a reduced bond strength. This extension of the Direct Stiffness Method is first briefly discussed, after which the implemented corrosion models are listed. In order to arrive at a safety format for the DSM tool, it is crucial to investigate the

propagation of typical uncertainties involved in the assessment of existing concrete structures.

Therefore, in this contribution, the abovementioned uncertainties are accounted for in the structural performance prediction using an extended DSM approach. It is investigated how the uncertainties on several types of input parameters influence the uncertainty on the outputs, i.e. the deformations, deflections, internal forces etc., applied on a deteriorating frame. Furthermore, the spatial distribution of these parameters is modelled using random fields. It is then investigated how the correlation lengths and correlation coefficients of several parameters influence the outputs of the DSM-tool. Finally, a sensitivity analysis is performed such that the parameters having the highest influence can be identified. Knowing these parameters is important for the life-cycle analysis of existing structures, more specifically in the decision making process regarding inspection techniques.

2. THE DIRECT STIFFNESS METHOD TOOL

The Direct Stiffness Method (DSM) is a well-known finite element method in the civil engineering field. It can be employed to relate the external forces acting on components such as beams and columns, to the displacements of these components through the use of a stiffness matrix. To accomplish this, the structure is divided into several elements connected at nodes. For each element, the constitutive relation can be written according to a local coordinate system, as given in Eq. (1).

$$\{F'\} = [S'] \cdot \{D'\} + \{F_0'\} \tag{1}$$

In this equation, $\{F'\}$ is a vector representing the element's nodal forces, i.e. the unknown internal forces acting on the nodes of the element. Furthermore, $[S']$ is the element's stiffness matrix, and the vector $\{D'\}$ contains the nodal displacements of the member according to the local coordinate system. Finally, the vector $\{F_0'\}$ contains the generalized forces on the element caused by external loads. For detailed expressions of these vectors and matrices, reference is made to Van Coile (2016).

2.1. The DSM tool

The Direct Stiffness Method is by default a linear, first order finite element method. In order to make more accurate structural assessments using this method, second order effects, material non-linearity and corrosion effects are added. This is accomplished by updating the stiffness of each element based on the constructed moment vs. curvature and normal force vs. strain diagrams, accounting for the corrosion effects. As a result, a DSM tool is constructed which is capable of executing more accurate performance predictions of existing RC structures. The implementation of second order effects and material non-linearity in the DSM tool has been further elaborated in Helderweirt et al. (2022).

2.2. Corrosion models

In existing concrete structures, corrosion is a common and important degradation phenomenon resulting in a number of interacting damage modes. These modes include the overall/local reduction of the steel area, cracking and spalling of the concrete cover due to the internal stresses arising from the corrosion products, modified constitutive material laws and a deteriorating bond between the steel reinforcement and the surrounding concrete (Coronelli and Gambarova, 2004). Overall, these effects lead to a reduction of the stiffness of reinforced concrete elements. Note that the DSM tool can easily be adjusted to accommodate other corrosion models than the ones described below.

2.2.1. Corrosion initiation and propagation

Generally, the corrosion process is described by two phases: the initiation phase and the propagation phase. In the propagation phase, the steel starts to corrode and the reinforcement area will decrease in time (Tuutti, 1982). Moreover, two types of corrosion can be distinguished: chloride-induced corrosion and carbonation-induced corrosion. In this contribution, chloride-induced corrosion will be considered, which leads

to more localized areas of depassivation (Coronelli and Gambarova, 2004).

The time until corrosion initiation as a result of chloride ingress can be modelled by Fick's second law of diffusion (fib, 2006):

$$T_i = \frac{1}{4D}\frac{c^2}{\left[\mathrm{erf}^{-1}\left(1-\frac{C_{cr}}{C_s}\right)\right]^2} \quad (2)$$

where D is the diffusion coefficient of chlorides penetrating into the concrete, c is the concrete cover, C_{cr} is the critical chloride concentration, C_s is the chloride concentration at the surface and $\mathrm{erf}^{-1}(.)$ is the inverse error function. After this time T_i, the propagation phase is initiated and the steel starts to corrode. As a result, the steel area decreases in function of time with a rate equal to the corrosion rate V_{corr} [mm/year]. The average reduction of the radius of the rebar P_{avg} can be described by Eq. (3).

$$P_{avg}(t) = V_{corr} \cdot (t - T_i) \quad (3)$$

However, in case of chloride-induced corrosion, localized pits occur of which the depths frequently exceed P_{avg}. The ratio of the maximum pitting depth to the average corrosion attack depth is given by the pitting factor R [-], which is assumed to be constant in time and ranges between 4 and 8 (Stewart, 2004). In this contribution, R is assumed deterministic and equal to 4. Based on this maximum pit depth, the corroded steel area can be calculated using e.g. the hemispherical corrosion model of Val and Melchers (1997). Finally, the corrosion degree α can be calculated as the ratio of the corroded steel area to the initial rebar section.

2.2.2. Corrosion cracking and spalling

The volume of corrosion products is larger than the initial steel volume (Tuutti, 1982). As a result, the internal pressure in the surrounding concrete increases which can result in concrete cracking and spalling.

In this contribution, the time between corrosion initiation and concrete cracking is modelled by the model proposed by Lv and Zhu (2016). After the concrete is considered cracked, the concrete will have a reduced strength which can be calculated according to Eq. (4) (Coronelli and Gambarova, 2004).

$$f_c^* = \frac{f_c}{1+K\frac{\varepsilon_1}{\varepsilon_{c0}}} \quad (4)$$

where K is related to the roughness and diameter of the rebars, and equals 0.1 for medium-diameter ribbed bars. ε_1 is the averaged tensile strain in the cracked concrete perpendicular to the applied compression and ε_{c0} is the strain at the peak compressive stress. Formulations of the latter can be found in Coronelli and Gambarova (2004).

In case spalling is observed, a conservative assumption is made and the entire concrete cover is neglected.

2.2.3. Reduced steel ductility

The corrosion process has shown to have a significant influence on the ductility of the steel rebars, especially in the presence of pits. This decrease in ultimate steel strain ε_{su} is modelled according to Eq. (5), based on the corrosion degree α (Zhu and François, 2013).

$$\frac{\varepsilon_{su,red}}{\varepsilon_{su}} = \begin{cases} e^{-0.1\alpha} & \alpha \leq 16\% \\ 0.2 & \alpha > 16\% \end{cases} \quad (5)$$

2.2.4. Reduced bond strength

Lastly, the reduced bond strength is considered in the extended DSM tool. The empirical model suggested by Bhargava et al. (2007) is adopted, which accounts for a constant value of the bond strength for lower corrosion degrees. For higher corrosion degrees, an exponential decrease is assumed according to Eq. (6), where $\tau_{b,max}$ designates the initial bond strength between concrete and steel, and $\tau^*_{b,max}$ represents the deteriorated bond strength.

$$\tau^*_{b,max} = \begin{cases} \tau_{b,max} & \alpha \leq 1.5\% \\ \tau_{b,max} \cdot 1.346\exp(-0.198\alpha) & \alpha > 1.5\% \end{cases} \quad (6)$$

In case the concrete strain is smaller than the steel strain due to insufficient bond, slip occurs, which results in an increased curvature in the cross-section. This increased curvature can be calculated considering an additional slip strain as proposed by Monti and Spacone (2000).

3. IMPLEMENTING UNCERTAINTIES IN THE DSM TOOL

The assessment of existing concrete structures involves dealing with uncertainties about both the material properties and the damage which might have occurred. Furthermore, the parameters describing the material properties and damage are not constant in time and space. The structural behaviour through time is incorporated through the time-dependent corrosion models, and the spatial variation is implemented in the DSM tool adopting random fields.

First, the distributions of the variables are listed and the spatial correlation structure is described. Next, the output of the DSM tool, i.e. deflections and internal forces, are analysed and it is investigated how the correlation structure affects the outputs.

3.1. Stochastic models for input variables

The stochastic models of all considered variables are listed in Table 1. The concrete tensile strength f_{ct} and E-modulus E_c are both calculated based on the concrete compressive strength f_c through equations (7) and (8) (JCSS, 2001). Additional variations in f_{ct} and E_c that are not well accounted for by the compressive strength are incorporated by means of the variables $Y_{f_{ct}}$ and Y_{E_c} respectively. The E-modulus of steel is assumed deterministic and equal to 205 GPa. (JCSS, 2001).

$$f_{ct} = 0.3 f_c^{2/3} \cdot Y_{f_{ct}} \quad (7)$$

$$E_c = 10.5 f_c^{1/3} \cdot Y_{E_c} \quad (8)$$

3.2. Modelling spatial correlation

The spatial variation of the input parameters is implemented by using random fields. Especially the chloride-induced corrosion process is known for highly localized pits, which implies the need to model these parameters as random fields rather than assuming they are constant over the entire structure. As a result, parameters such as the corrosion rate are considered to vary over the structure, leading to high differences in corrosion degrees between the subelements. The discretisation of the Gaussian random fields can be done using the Karhunen-Loève decomposition, as described by Sudret and Der Kiureghian (2000). In the case of non-Gaussian fields, the Nataf transformation is used to model these fields by an underlying Gaussian field.

The correlation model used in this contribution is the squared exponential correlation model, described by Eq. (9) (Sudret and Der Kiureghian, 2000). Note that the tool can easily be adjusted to use other correlation models as well.

$$\rho(x, x') = \rho_0 + (1 - \rho_0) \exp\left(-\frac{\Delta^2}{L_c^2}\right) \quad (9)$$

In Eq. (9), $\rho(x, x')$ describes the correlation between location x and x' in the same structural

Table 1: Stochastic models (Holický, 2009), (JCSS, 2001), (fib, 2006), (Duracrete, 2000), JCSS (2001), Stewart and Mullard (2007), Straub (2011)

Parameter	***Description***	***Distr.*****	***Mean μ***	***Std. σ***	ρ_0 **[-]**	ρ_e **[-]**	L_c **[m]**
f_c [MPa]	*Concrete compressive strength*	*LN*	*42.85*	*6.43*	0.2	0.5	5.0
Y_{fct} [-]	*Model uncertainty concrete tensile strength*	*LN*	*1*	*0.30*	0.2	0.5	5.0
Y_{Ec} [-]	*Model uncertainty concrete E-modulus*	*LN*	*1*	*0.15*	0.2	0.5	5.0
f_y [MPa]	*Steel yield strength*	*N*	*460*	*30*	1.0	0.4	10.0
A_s [mm²]	*Steel reinforcement area*	*N*	$A_{s,nom}$	*0.02μ*	*n/a*	*n/a*	*n/a*
c [mm]	*Concrete cover*	*B(0;3μ)*	*40*	*5*	0.2	0.5	3.5
ε_{su} [-]	*Ultimate steel strain*	*N*	*0.12*	*0.02*	*n/a*	*n/a*	*n/a*
D [mm²/ year]	*Diffusion coefficient of concrete*	*LN*	*20*	*10*	0.2*	0/0.2*	2.0*
C_s [wt.-%/c]	*Surface chloride concentration*	*LN*	*2*	*0.9*	0.2*	0/0.2*	2.0*
C_{cr} [wt.-%/c]	*Critical chloride concentration*	*LN*	*0.6*	*0.15*	0.2*	0/0.2*	2.0*
V_{corr} [mm/ year]	*Mean corrosion rate*	*LN*	*0.03*	*0.02*	0.2*	0/0.2*	2.0*

** Values used for the basic case, which are altered in the parameter study (cf. infra).*
*** N: Normal distribution, LN: Lognormal distribution, B(a,b): Beta distribution with lower bound a and upper bound b*

component. Furthermore, ρ_0 denotes the lower bound for the correlation, Δ is the distance between locations x and x' and L_c is the correlation length. For two locations in different structural components (e.g. beam and column), a constant correlation ρ_e is assumed.

In Table 1, the correlation lengths and coefficients are summarized for each parameter which is modelled as a random field. All other parameters are assumed constant within each structural component, as their spatial variation is assumed to be limited (JCSS, 2001). In subsequent sections, the correlation coefficients and correlation lengths of the corrosion properties are altered to show their influence on the outputs of the DSM tool.

For corrosion properties, an external correlation coefficient of 0.2 is adopted for structural members exposed to similar environmental conditions and 0 for members exposed to different environmental conditions.

4. APPLICATION EXAMPLE: RC FRAME

In this section, it is investigated how the uncertainties and spatial correlation defined in section 3 propagate through the DSM tool, by means of a reinforced concrete frame. The frame, shown in Figure 1, consists of two clamped columns and one beam. The frame is subdivided in 30 elements of 0.5 m long. The concrete quality is C30/37, and the steel reinforcement has a yield strength of 400 MPa. Furthermore, the columns have a cross section of 600 x 600 mm and are reinforced by 4 bars with diameter 20 mm. The beam has a height and width of 600 mm and 300 mm, respectively, and has bottom and top reinforcement of 6 bars with diameter 12 mm. Lastly, the nominal value of the concrete cover is 40 mm.

The frame is loaded by a horizontal point load F, with a mean value of 25 kN and a standard deviation of 5 kN, and a uniformly distributed load p, with a mean and standard deviation of 10 kN/m and 2 kN/m, respectively. Both forces follow a Gumbel distribution. Lastly, the correlation structure is as described in Table 1, with an external correlation for the corrosion variables of 0.2 between the two columns, and 0 between the columns and the beam.

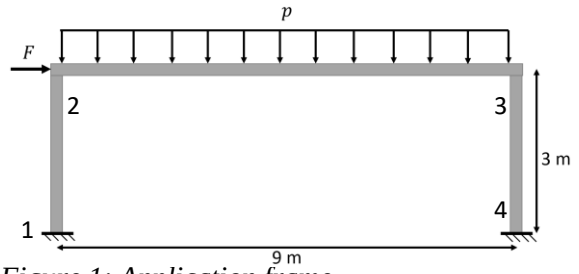

Figure 1: Application frame

4.1. Output of the extended DSM tool

The extended DSM tool is used to calculate the response of the frame for different time steps. Uncertainties are accounted for based on 200 Latin Hypercube Samples (LHS) drawn from the distributions presented in section 3. Consequently, histograms of the deformations, internal forces, strains, curvatures etc., at each time step are obtained.

In Figure 2, the calculated corrosion degree of the top reinforcement at midspan of the beam is given. This is the average corrosion degree over all rebars in the top of the cross-section. In this histogram, all cases where no corrosion was found are left out, and represented by the probability of 0% corrosion, which is 51% in all cases. The probability of obtaining a corrosion degree below 10% is 76%.

The histogram of the deflection at midspan of the beam is shown in Figure 3. As can be seen here, a bimodal behaviour appears, which can be explained by looking at the cracking behaviour: in case the concrete remains uncracked in the entire frame, the deflections are relatively limited. However, when the cracking moment is exceeded, flexural cracks occur which lower the overall stiffness of the frame, resulting in significantly higher deformations. Furthermore, the histogram can be fitted by two weighed lognormal distributions, as done in Botte et al. (2021). Figure 4 then shows this displacement in function of time, represented by three lines: two lines corresponding to the mean value of both distributions of the bimodal fit, together with their

95% confidence intervals, and one line representing the 95% fractile of the entire distribution. As can be seen, the deflections increase through time due to the corrosion process, along with their uncertainties.

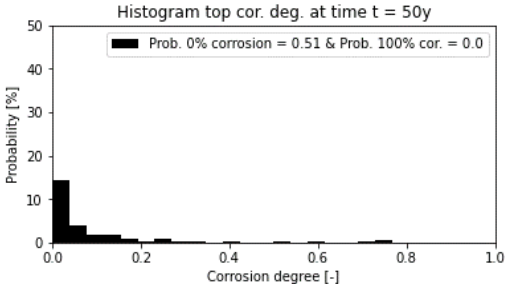

Figure 2: Histogram of the calculated corrosion degree in the top reinforcement of the beam at midspan after 50 years.

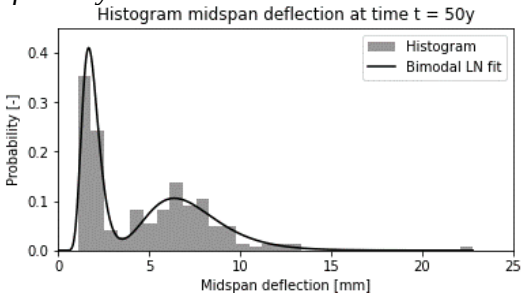

Figure 3: Histogram of the calculated deflections in the beam at midspan after 50 years.

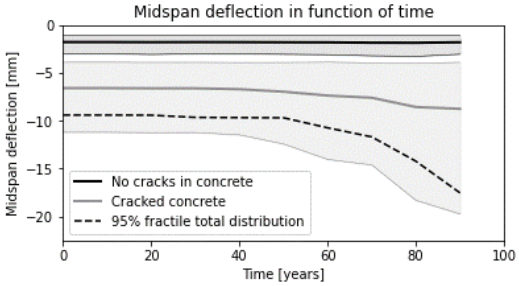

Figure 4: Midspan deflection in function of time with.95% fractile.

Finally, the internal forces are studied in terms of the bending moments (Figure 5). For each sub element, a histogram of the bending moments is constructed. These histograms can be fitted by a normal distribution, and Figure 5 shows the 95% confidence interval of the moment line in the entire frame. It should be noted that the sign convention for the bending moments in the DSM tool is defined by the order in which the nodes are numbered. In this case, the numbering is as in Figure 1, resulting in a convention that is different in sign for the two columns.

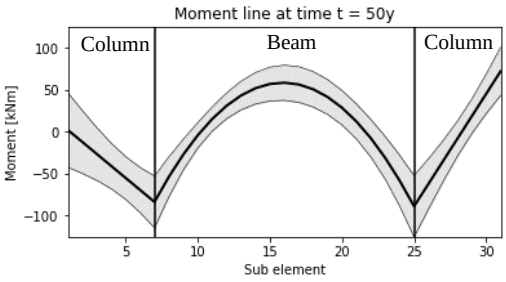

Figure 5: Calculated moment line with 95% confidence interval

4.2. Parameter study on the correlation structure of the corrosion parameters

The outcomes of previous example are obtained by using the correlation parameters as described in Table 1. In this section, a parameter study is performed to see the influence of these parameters on the structural reliability of the most critical element.

The influence of the correlation structure on the reliability index of the frame can be derived from the outputs of the DSM tool. As an example, the reliability index of the most critical element for flexural failure is given in Figure 6, for increasing correlation lengths of parameters D, C_s, C_{cr} and V_{corr} (indicated with * in Table 1). The other parameters are kept constant as described in Table 1. The most critical element is the outmost right sub element of the beam, as the moment line is highest there (Figure 5). To determine this value, for each LHS sample, the acting moment M_E is subtracted from the resisting moment M_R. The latter is calculated as the ultimate moment in the constructed moment vs. curvature diagram, accounting for the corrosion effects. Consequently, samples for the limit state variable $Z = M_R - M_E$ are obtained, which are fitted by a normal distribution. The probability of failure P_f is consequently calculated as the probability that Z yields negative values. Finally, the reliability index β is obtained using $\beta = -\Phi(P_f)$. As can be seen in this figure, the importance of the correlation length on the safety index of the structural member remains limited. At year 0, when corrosion does not yet affect the structural response, a scatter in the safety index can be seen. This spread on the results remains

more or less constant throughout the years, showing a minimal influence of the correlation length on the safety of the most critical element.

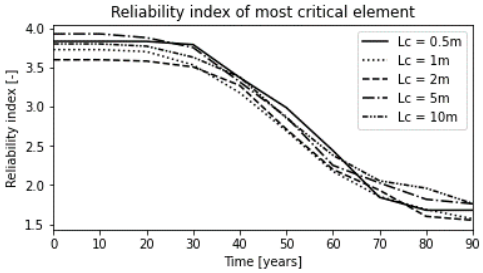

Figure 6: Reliability index of the most critical element for different correlation lengths.

Next, the influence of ρ_0 and ρ_e is investigated. In Figure 7 and Figure 8, the reliability of the most critical component are given for correlation coefficients ρ_0 and ρ_e ranging from 0 to 1 for parameters D, C_s, C_{cr} and V_{corr}. Again a limited influence of ρ_0 and ρ_e is found, as the spread on the results remains more or less constant through time.

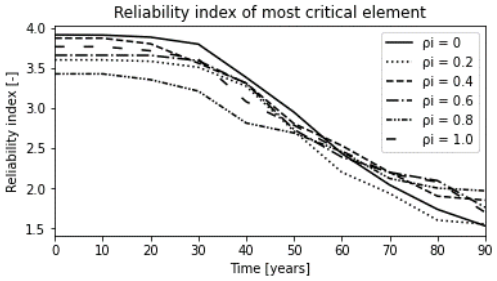

Figure 7: Reliability index of the most critical element for different correlation coefficients.

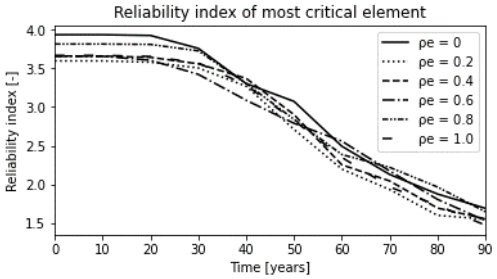

Figure 8: Reliability index of the most critical element for different external correlation coefficients.

4.3. Sensitivity study on the input variables

Lastly, the influence of each input parameter on the midspan deflection is investigated based on Sobol indices (Saltelli, 2002). The results are summarized in Figure 9, for different time steps. The higher the Sobol index, the more influence the parameter has on the midspan deflection.

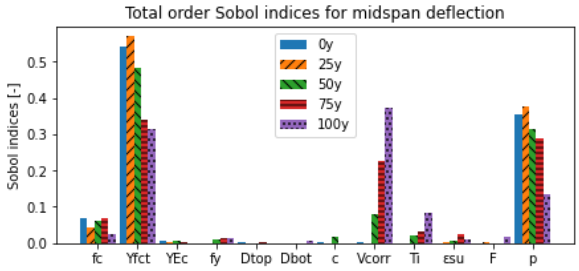

Figure 9: Total order Sobol indices for the midspan deflection.

As can be seen in Figure 9, the parameters having the highest influence on the midspan deflection are the concrete tensile strength f_{ct} and the uniformly distributed load p. The high influence of the tensile strength can be explained by the bimodal behaviour of the deflections: for lower tensile strengths, the concrete cracking moment is lower, resulting in higher deflections and vice versa.

Furthermore, the older the structure, the more important the corrosion parameters become, such as the corrosion rate V_{corr} and initiation period T_i. This is due to the corrosion process being a time-dependent process which results in more damage over time, leading to a higher influence on the performance prediction for older structures.

5. CONCLUSIONS

In this contribution, an extended DSM tool is used to perform a probabilistic analysis of a reinforced concrete frame. First, this extended Direct Stiffness Method tool was described. The advantage in using this DSM tool, is that no advanced FE models need to be constructed to assess existing RC structures. After that, the uncertainties typically involved in the assessment of existing structures were added to the model, including their spatial variability. It was then applied on a RC frame, for which the corrosion degree, internal forces and deformations could be calculated in function of time. Furthermore, it was found that the midspan deflections could be fitted by a bimodal lognormal distribution.

Next, a parameter study was done on the correlation structure of the corrosion parameters. In general, it was found that the correlation variables had little to no influence on the safety index of the most critical element of the frame.

Finally, a sensitivity analysis was performed on all input variables. It was found that the concrete tensile strength and the uniformly distributed load had the highest influence on the midspan deflections. Furthermore, the corrosion properties become more significant through time, as the corrosion process becomes more significant in the structural response near the end of the structure's lifetime. Knowing these parameters is of importance to determine which measurements will be the most effective in reducing the overall uncertainty on the performance prediction. This plays an important role in the decision making process regarding inspection strategies, leading to a more efficient life-cycle methodology of existing RC structures.

ACKNOWLEDGEMENTS

This research was performed within the framework of project lifeMACS "Multi-layer Bayesian life-cycle Methodology for the Assessment of existing Concrete Structures", supported by FWO-Flanders (FWO-SBO project S001021N).

REFERENCES

Bhargava, K., Ghosh, A., More, Y., & Ramanujam, S. (2007). Corrosion-induced bond strength degradation in reinforced concrete - Analytical and empirical models. *Nuclear Engineering and Design, 237*(11), 1140-1157.

Botte, Wouter, Didier Droogné, and Robby Caspeele. (2021). "Reliability-Based Resistance of RC Element Subjected to Membrane Action and Their Sensitivity to Uncertainties." *Engineering Structures* 238.

Coronelli, D., & Gambarova, P. (2004). Structural Assessment of Corroded Reinforced Concrete Beams: Modeling Guidelines. *Journal of Structural Engineering, 130*(8), 1214-1224.

Duracrete. (2000). *DuraCrete – Probabilistic Performance based Durability Design of Concrete Structures.*

fib. (2006). *fib Bulletin 34: Model code for service life design*, Lausanne.

Helderweirt, S., Van Den Hende, K., Botte, W., Verstrynge, E., & Caspeele, R. (2022). Development of a stepwise adjusting direct stiffness method approach for the assessment of existing concrete structures. *Proceedings for the 6th fib International Congress 2022*, 2150–2159.

Holický, M. (2009). *Reliability Analysis for Structural Design.*

JCSS. (2001). *Probabilistic Model Code*.

Lv, Q., & Zhu, R. (2016). Model for Forecasting the Time of Corrosion-induced Reinforced Concrete Cracking. *Proceedings of the 2nd International Conference on Performance-based and Life-Cycle Structural Engineering (PLSE 2015)*.

Monti, G., & Spacone, E. (2000). Reinforced Concrete Fiber Beam Element with Bond-Slip. *Journal of Structural Engineering, 126*(6), 654-661

Saltelli, A. (2002). Making best use of model evaluations to compute sensitivity indices. *Computer Physics Communications, 145*, 280-297.

Stewart, M. G. (2004). Spatial variability of pitting corrosion and its influence on structural fragility and reliability of RC beams in flexure. *Structural Safety, 26*(4), 453-470.

Stewart, M., & Mullard, J. (2007). Spatial time-dependent reliability analysis of corrosion damage and the timing of first repair for RC stuctures. *Engineering Structures*, 1457-1464.

Straub, D. (2011). Reliability updating with inspection and monitoring data in deteriorating reinforced concrete slabs. *Proceedings of ICASP11 – Application of Statistics and Probability in Civil Engineering*, 2309-2316

Sudret, B., & Der Kiureghian, A. (2000). *Stochastic finite element methods and reliability: A state-of-the-art report.*

Tuutti, K. (1982). *Corrosion of steel in concrete.* Stockholm: Swedish Cement and Concrete Research Institute.

Val, D. V., & Melchers, R. E. (1997). Reliability of Deteriorating RC Slab Bridges. *Journal of Structural Engineering, 123*(12), 1638-1644.

Van Coile, R. (2016). *Towards reliability-based structural fire safety: development and probabilistic applications of a direct stiffness method for concrete frames exposed to fire.* Ghent University Academic Bibliography.

Zhu, W., & François, R. (2013). Effect of corrosion pattern on the ductility of tensile reinforcement extracted from a 26-year-old corroded beam. *Advanced Concrete Constructions, 1*, 121-136.